



Gazi University

**Journal of Science**

PART A: ENGINEERING AND INNOVATION

<http://dergipark.org.tr/gujisa>

## Prediction of Immediate Deflections for RC Beams Using Stress-varying Modulus of Elasticity

Eray ÖZBEK<sup>1\*</sup> <sup>1</sup>Gazi University, Engineering Faculty, Civil Engineering Department, 06570 Ankara, Türkiye

Keywords	Abstract
Beam	This paper discusses the immediate deflection calculation of reinforced concrete beams and their consistency with the experimental results. For this purpose, a total of six T-beams with low, medium, and high reinforcement ratios were tested and then, deflection behavior was compared with the well-known Branson (1965) and Bischoff (2005) approaches. Although both approaches could yield close results for the low reinforcement at service loads by using a constant modulus of elasticity, they underestimated the deflections of medium and highly reinforced beams. Thus, the nonlinear behavior of concrete that changes with stress was also considered in the subsequent analyzes. As a result, the developed new approach could predict the experimental deformations very accurately, especially at the level of service loads.
Deflection	
Serviceability	
Elastic Modulus	
Concrete Model	

### Cite

Özbek, E. (2022). Prediction of Immediate Deflections for RC Beams Using Stress-varying Modulus of Elasticity. *GU J Sci, Part A, 9(4)*, 516-525.

Author ID (ORCID Number)	Article Process	
E. Özbek, 0000-0001-6738-7789	<b>Submission Date</b>	27.10.2022
	<b>Revision Date</b>	25.11.2022
	<b>Accepted Date</b>	28.11.2022
	<b>Published Date</b>	31.12.2022

## 1. INTRODUCTION

As known, reinforced concrete (RC) structural members are designed to resist loads without experiencing failure. On the other hand, RC members should also meet serviceability requirements to assure proper behavior and functionality under these loads. Deflections and cracking properties are the major concerns that can affect serviceability. Therefore, it is very crucial to predict these features with an estimate close to the actual behavior. However, this is not straightforward due to the specific behavior of RC. The flexural stiffness of a beam section depends on the moment of inertia normal to loading direction and the modulus of elasticity. However, the product of both variables is not constant for RC beams at any stage of the loading. Nonlinear and time-dependent stress-strain behavior of concrete results variability in the modulus of elasticity. On the other hand, the moment of inertia significantly changes after cracking and keeps changing due to crack propagation.

Accordingly, many research was conducted to calculate or predict immediate deflections of RC beams. They dealt with predicting the decreasing trend of moment of inertia due to cracked section properties. This behavior was taken into account by using different effective moment of inertia at corresponding load levels. Among these studies, Branson (1965) became very popular and conventional. This approach was also adopted by Turkish Standards TS500 (2000), American Concrete Institute, ACI 318-14 (2014), Canadian Standards CSA (2004), AASHTO (2005), Australian Standards, AS 3600-2009 (2009). American Concrete Institute Building Codes had been using this approach for more than 35 years (Mancuso & Bartlett, 2017). However, in 2019, ACI 318-19 (2019) removed the Branson (1965) equation, and instead adopted the Bischoff (2005) approach. The method proposed by Bischoff (2005) slightly better estimated the load-deflection of RC beams with a more rational approach of cracking behavior (Kalkan, 2010; Mancuso & Bartlett, 2017; Bischoff, 2020).

\*Corresponding Author, e-mail: [erayozbek@gazi.edu.tr](mailto:erayozbek@gazi.edu.tr)

The current study was conducted to estimate the immediate deflection of RC beams. For this purpose, half-scaled and T-sectioned RC beams with the reinforcement ratios of high, medium, and low were tested under monotonic loads. Afterwards, obtained experimental load-deflection relationships were compared with analytical ones proposed by Branson (1965) and Bischoff (2005) in accordance with the ACI 318-14 (2014) and ACI 318-19 (2019), respectively. Both methods gave quite close results to experimental values for the beams with low reinforcement ratio. However, they underestimated the deflections of medium and highly reinforced beams especially at service load levels. In other words, this is on the unsafe side. The latest research are still mainly focused on cracking behavior of RC members and estimating the effective moment of inertia. Consequently, sophisticated methods have been developed (Ammash et al., 2018; Arabshahi et al., 2022). In these approaches, even shear deformations were considered and taken into account (Kim et al., 2021). On the other hand, the effect of the elastic modulus of the concrete, which shows non-linear behavior with stress, was omitted. In other words, the specific behavior for one of the two main parameters affecting flexural stiffness is neglected in the calculations as far as the author knows. ACI 318-14 (2014) and ACI 318-19 (2019) permit to use a constant modulus of elasticity for these analyses. Thus, the nonlinear behavior of concrete that changes with stress was also considered in the subsequent analyzes to predict deflections as accurately as possible. The widely-accepted Hognestad (1951) concrete model was implemented into the calculations in order to reflect the effect of an elasticity modulus that changes with stress. Obtained results were presented graphically and discussed in terms of accuracy.

## 2. MATERIAL AND METHOD

### 2.1 Experimental Research

A set of ½ scaled and T-sectioned six RC beams were tested under monotonic four-point bending. Table 1 indicates the basic properties of these specimens. Dimensions and materials of the beam specimens were designed considering common practice and the experimental test setup limits. Ratio of the longitudinal reinforcement and flange thicknesses were selected as research parameters. Concrete of the specimens were cast monolithically. Figure 1 shows the dimensions and reinforcement detailing of the test specimens. The length of the RC beams was 3000 mm. The beam width, depth, and flange width of beams were 125/250/725 mm, respectively. Flange thickness was 100 or 75 mm based on the specimen type. For each specimen, the upper flange region was reinforced by orthogonally placed Ø5/75 (rebar diameter is 5 mm and center to center spacing is 75 mm) rebars. On the other hand, while the bottom region of the flange was reinforced with Ø5/75 for the longitudinal direction, the transverse direction was Ø5/150. Five millimeters of net concrete cover distance was adopted for the flange reinforcement.

*Table 1. Test specimen properties*

Specimen	Flange thickness (mm)	Compression rebars	Tension rebars	Reinforcement ratio (%)	
L75	75	2Ø8	3Ø8	low	0.51
M75	75	2Ø10	4Ø10	medium	1.07
H75	75	2Ø12	4Ø12	high	1.55
L100	100	2Ø8	3Ø8	low	0.51
M100	100	2Ø10	4Ø10	medium	1.07
H100	100	2Ø12	4Ø12	high	1.55

RC beams in this study were formed with three main longitudinal tension reinforcement ratios, which are low, medium, and high. Accordingly, beams with low reinforcement had 3Ø8 (3 rebars with a diameter of 8 mm) tension and 2Ø8 compression, medium reinforcement had 4Ø10 tension and 2Ø10 compression, high reinforcement had 4Ø12 tension and 2Ø12 compression rebars. Numerical expression of these tension reinforcement ratios were indicated in Table 1. Ten millimeters of net concrete cover was left for longitudinal rebars. Transverse reinforcement was detailed by double-legged stirrups of Ø5/100 mm which had 60 mm long 135° bended hooks. Stirrup detailing was kept the same along the length of all specimens. Transverse reinforcement was designed to prevent shear failures in the experiments.

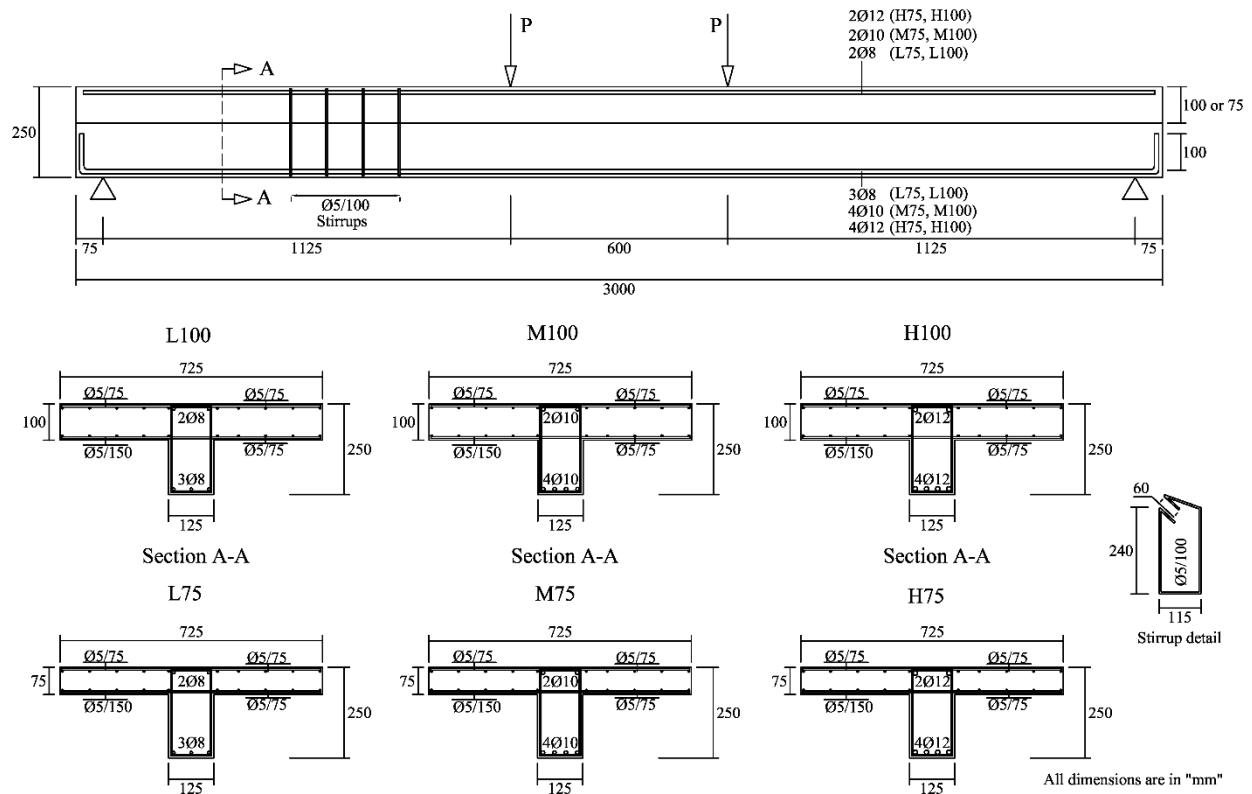


**Figure 1.** Dimensions and detailing of test specimens

Low and high longitudinal tension reinforcement ratios for the test specimens were designed according to TS500 (2000). While the low one corresponds to the minimum ( $\rho_{min}$ ), the high one corresponds to the maximum ( $\rho_{max}$ ) longitudinal reinforcing limits for flexural members and calculated by Eq. (1) and Eq. (2).

$$\rho_{min} = 0.8 \frac{f_{ctd}}{f_{yd}} \quad (1)$$

$$\rho_{max} = 0.85\rho_b \leq 0.02 \quad (2)$$

where  $f_{yd}$  is the design yield strength of longitudinal rebars and obtained by dividing characteristic strength to material factor of 1.15;  $f_{ctd}$  is the design tensile strength of concrete and obtained by dividing characteristic strength to material factor of 1.5;  $\rho_b$  is the reinforcement ratio for the balanced section. The medium reinforcement ratio was set by the arithmetic mean of these maximum and minimum boundaries.

The name of the specimens were determined to represent their test parameters. Accordingly, the first letter (H, M, or H) refers to the low, medium, and high reinforcement ratios by their initials. The following number indicates the flange thickness of the beam in millimeters as 75 or 100 (Table 1).

Concrete compressive strengths were determined based on standard 150×300 mm cylinder tests conducted on the 28th day of the casting. The same concrete mixing ratio was used for all specimens and there was not any chemical additives in it. At least ten concrete cylinder specimens were tested for each RC beam. Accordingly, the mean concrete compressive strength ( $f_c$ ) of the concrete was calculated as 15.8 MPa, with a sample standard deviation of 0.63 MPa. Ribbed steel bars were used for the reinforcement. However, while Ø5 rebars were in S500 grade, Ø8, Ø10, and Ø12 rebars were in S420 grade. While S500 grade has a minimum yield strength ( $f_y$ ) of 500 MPa and an ultimate strength ( $f_{su}$ ) of 550 MPa, these values for S420 grade are 420 MPa and 500 MPa, respectively.

The experimental set-up was illustrated in Figure 2. Accordingly, RC beams were placed on simple supports. Tests were conducted in the closed steel frame. The load was acted by a hydraulic jack, and this load transmitted to the RC beam with the help of load-spreader steel shapes. The upper steel beam was utilized to divide the main load into halves. This simple supported steel beam had a clear span length of 600 mm and was standing on two steel shapes which were located on transverse direction of the RC beam. In this way, two uniformly distributed loads acted along the transverse direction of the test specimen. To ensure more even load distribution, rubber pads were also placed between the steel shapes and the RC beam. The acting force was measured by a canister type load cell which was attached to the hydraulic jack. The load cell had an accuracy of 0.25%. Linear variable differential transformers (LVDTs), which had an accuracy of 0.1%, were utilized to measure vertical displacements at the mid-span, loading projections, and supports. Since observed support settlements during the experiments were very close to zero, they were neglected during net displacement calculations. The vertical displacements measured from the loading projections were for curvature calculations and also a backup for the mid-span measurement. Monotonic quasi-static load was maintained up to 150 mm, which is the stroke length capacity of the hydraulic jack or a significant (at least 15%) decrease in the maximum load. All specimens experienced ductile flexural failure as expected. There was no sign of shear or bond damage. The experimental load-deflection diagrams of RC beams were plotted and shown in Figure 3 for comparison. In these diagrams, while the deflection axis corresponds to the net mid-span deflection, the load axis corresponds to the force measured by the load cell.

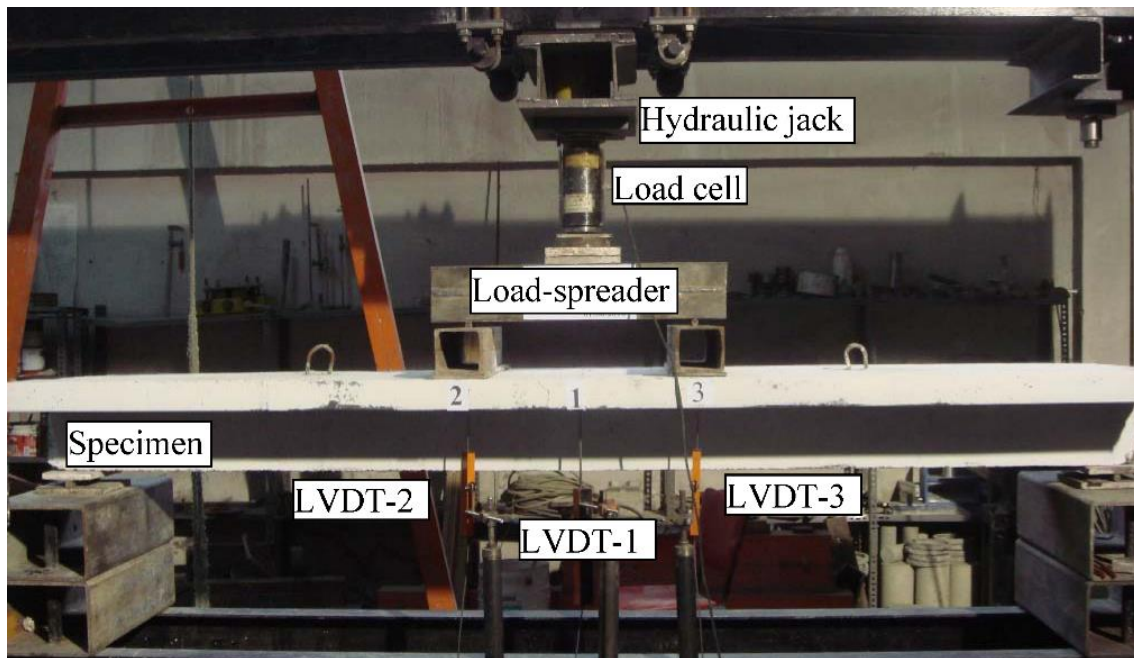


Figure 2. Test set-up

## 2.2 Analytical Study

Consecutively, the following steps were taken for predicting analytical load-deflection curves of the tested RC beams according to both methods developed by Branson (1965) and Bischoff (2005). Initially, the rupture modulus of concrete ( $f_r$ ) was computed as 2.4 MPa by using the Eq. (3) according to (ACI 318-19, 2019):

$$f_r = 0.62\lambda\sqrt{f'_c} \quad (3)$$

where  $\lambda$  is the lightweight concrete modification factor to account for the decreased mechanical properties and in this case  $\lambda = 1$ ,  $f'_c$  is the specified compressive strength of concrete in MPa and was taken as 15 MPa based on cylinder tests.

The cracking moment ( $M_{cr}$ ) was computed for the beams by the following Eq. (4) (ACI 318-19, 2019).

$$M_{cr} = \frac{f_r I_g}{y_t} \quad (4)$$

where  $y_t$  is the distance between gross section neutral axis and extreme fiber in tension,  $I_g$  is the gross-section moment of inertia by neglecting reinforcement.  $I_g$  was calculated as 325055499 mm<sup>4</sup> and 328342608 mm<sup>4</sup> for the beams with the flange thickness of 75 and 100 mm, respectively. Calculated  $M_{cr}$  values were explicitly given in Table 2.

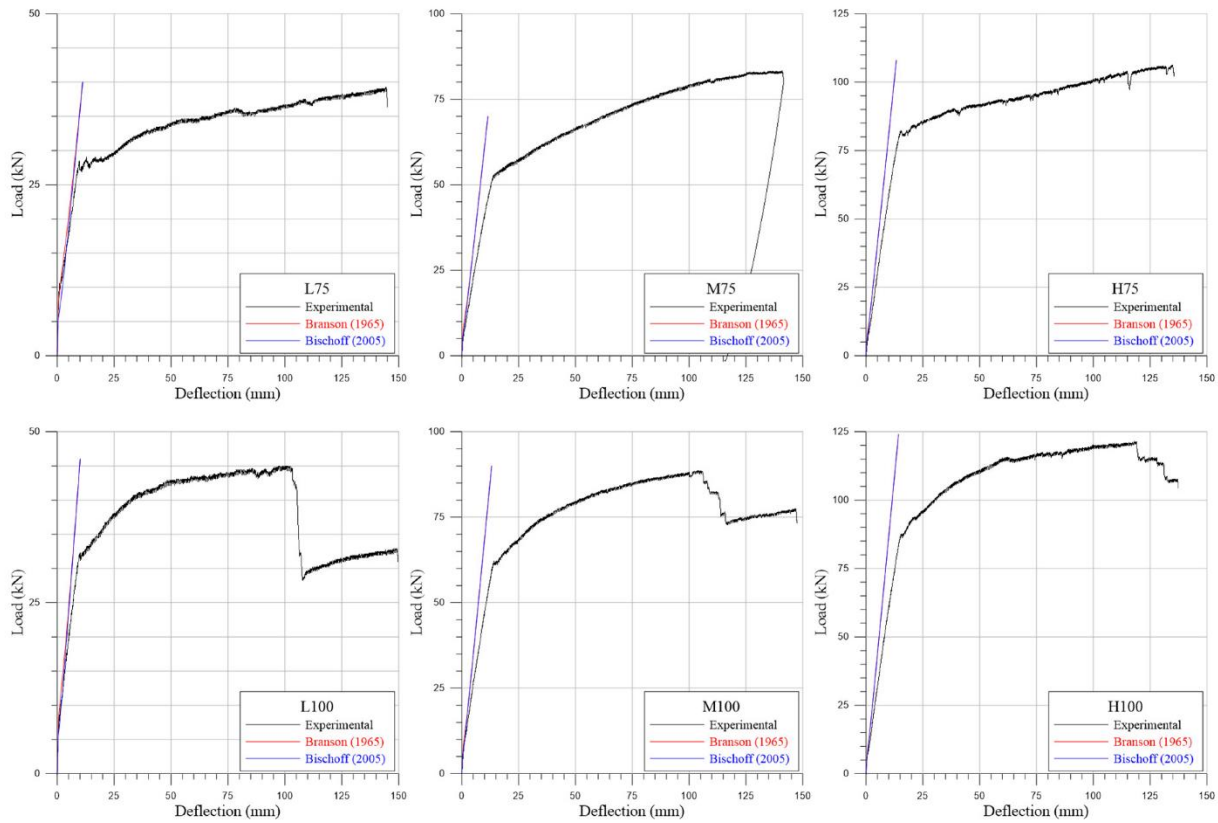


Figure 3. Analytical and experimental load-deflection diagrams

Table 2. Used values for analytical approach

Specimen	Tension reinforcement area (mm <sup>2</sup> )	Compression reinforcement area (mm <sup>2</sup> )	$I_{cr}$ (mm <sup>4</sup> )	$y_t$ (mm)	$y_c$ (mm)	$M_{cr}$ (kNmm)
L75	151	101	87601792	176.6	41.6	4416.5
M75	314	157	151440468	176.6	47.6	4416.5
H75	452	226	201074095	176.6	52.0	4416.5
L100	151	101	112361382	174.3	51.7	4520.7
M100	314	157	170151410	174.3	56.0	4520.7
H100	452	226	215662224	174.3	59.2	4520.7

The procedures for Branson (1965) and Bischoff (2005) methods are the same up to this stage. However, according to Branson (1965), if the RC member is cracked at one or more sections, immediate deflections should be calculated with the effective moment of inertia ( $I_e$ ) given in Eq. (5) (ACI 318-14, 2014). On the other hand, according to Bischoff (2005), if the acting moment ( $M_a$ ) is less than or equal to  $2/3M_{cr}$ ,  $I_e$  can be taken equal to  $I_g$ . Otherwise, the following Eq. (6) should be used, if  $M_a$  is greater than  $2/3M_{cr}$  (ACI 318-19, 2019).

$$I_e = \left(\frac{M_{cr}}{M_a}\right)^3 I_g + \left[1 - \left(\frac{M_{cr}}{M_a}\right)^3\right] I_{cr} \leq I_g \quad (5)$$

$$I_e = \frac{I_{cr}}{1 - \left(\frac{(2/3)M_{cr}}{M_a}\right)^2 \left(1 - \frac{I_{cr}}{I_g}\right)} \quad (6)$$

where  $I_{cr}$  is the cracked section moment of inertia which transformed in terms of concrete,  $I_g$  is the moment of inertia of gross concrete section about centroidal axis, neglecting reinforcement;  $M_a$  is the maximum moment acting on the RC member at stage deflection is calculated.  $I_{cr}$  was computed according to the derivations in ACI 435R-95 (2000) and shown for each specimen in Table 2. The elastic modulus of concrete ( $E_c$ ) was computed according to ACI 318-19 (2019) and found as 18203 MPa by Eq. (7). Elastic modulus of the steel rebars ( $E_s$ ) were taken as 200000 MPa.

$$E_c = 4700 \sqrt{f'_c} \quad (7)$$

The following remaining procedures were applied to obtain the analytical load-deflection diagrams of the RC beams by both mentioned methods. Since measured deflections only include applied load, deflection resulted from self-weight was neglected. Acting load was started from zero and increased by 0.5 kN steps until the maximum load values in the experiments were achieved. Load steps were expressed in terms of  $M_a$  at the mid-span. Thus,  $I_e$  was computed for each  $M_a$  value by operating the protocols specific to each method.

Typical Eq. (8) was derived for computation of mid-span deflection ( $\delta$ ) for a simple supported beam subjected to two symmetrical concentrated loads. In the Eq. (8),  $P$  is one of the two acting concentrated loads and is equal to half of the total applied load;  $a$  is the shear span length which in this case equal to 1125 mm;  $L$  is the net span length and equal to 2850 mm for the current test set-up (Figure 1).

$$\delta = \frac{P a}{24 E_c I_{ef}} (3L^2 - 4a^2) \quad (8)$$

Eventually, analytical load-deflection diagrams were drawn and presented with the experimental corresponding ones in Figure 3.

### 2.3 Proposed Method

In the proposed method, Eq. (6) which is adopted by ACI 318-19 (2019) was used as it is, except for the constant  $E_c$  assumption. As known, since the stress-strain behavior of concrete is nonlinear, it is possible to determine different  $E_c$  value for each point on the curve. The deviation from linearity becomes more obvious with increasing stress. Various models have been developed to express stress-strain relationship of concrete analytically (Hognestad, 1951; Hognestad et al., 1955; Desayi & Krishnan, 1964; Todeschini et al., 1964; Popovics, 1973; Carreira & Chu, 1985; Kumar, 2004). Among these, the widely-accepted Hognestad (1951) model with the Eq. (9) given below was selected for its convenience.

$$\sigma_c = f'_c \left[ \frac{2\varepsilon_c}{\varepsilon_{co}} - \left( \frac{\varepsilon_c}{\varepsilon_{co}} \right)^2 \right] \text{ for } \varepsilon_c \leq \varepsilon_{co} \quad (9)$$

where  $\sigma_c$  is the stress in concrete;  $\varepsilon_{co}$  is the strain corresponding with the maximum stress  $f'_c$ ;  $\varepsilon_c$  is the strain in which the stress is computed. If  $\varepsilon_c = \sigma_c / E_c$  is substituted in the Eq. (9), and then solved for  $E_c$ , following Eq. (10) can be obtained for the valid root. Thus,  $E_c$  could be defined as a secant modulus for each  $\sigma_c$  value.

$$E_c = \frac{f'_c [1 + \sqrt{1 - (\sigma_c / f'_c)}]}{\varepsilon_{co}} \quad (10)$$



In Eq. (10),  $\varepsilon_{co}$  was taken as 0.002 which is valid for most of the cases (CEB-FIB, 1970).  $f_c'$  was 15 MPa based on cylinder tests.  $\sigma_c$  was calculated for each  $M_a$  value according to the adopted practical approach by Eq. (11).

$$\sigma_c = \frac{M_a y_c}{I_e} \quad (11)$$

where  $y_c$  is the distance between neutral axis and the extreme fiber in compression. The value of  $y_c$  was calculated by the derivations of flanged sections with compression steel based on the ACI 435R-95 (2000) and given for each specimen explicitly in Table 2.  $I_e$  was computed by Eq. (6) which is Bischoff (2005) approach due its more rational results than the Branson (1965).

In this way, the analytical load-deflection diagram of the specimens plotted by using stress-varying modulus of elasticity were illustrated in Figure 4 with the previously drawn ones in Figure 3. Note that some portions of the post-yielding experimental curves were removed in order to make precise evaluations on a larger scale.

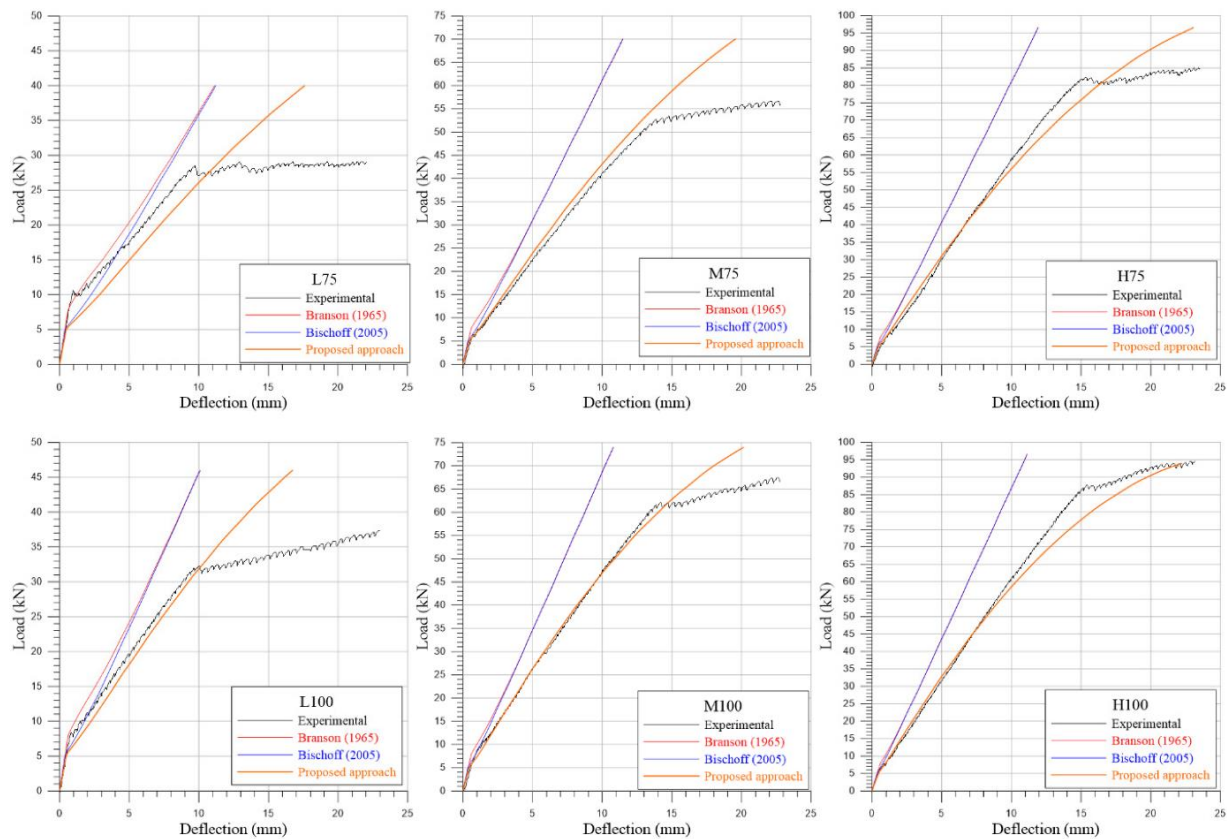


**Figure 4.** Initial load-deflection curves including proposed ones

### 3. RESULTS AND DISCUSSION

First point of the slope change in the load-deflection diagrams corresponds to the cracking load of the RC beams (Figure 4). Branson (1965) and Bischoff (2005) equations mostly underestimated the deflections after cracking. The deviation was more obvious for the medium and high reinforcement ratios (Figure 3). Exceptionally, Bischoff (2005) method slightly overestimated deformations up to approximately 1.5 times the experimental cracking load for beams with low reinforcement ratios (Figure 4). While Branson's (1965) approach was better for estimating the cracking behavior in RC beams with low reinforcement ratios, Bischoff's (2005) was better for medium and highly reinforced beams. Both methods resulted in almost equal deflections after about 2.5 times the experimental cracking loads. Therefore, the effects of the methods on behavior were dominant only for beams with low reinforcement. On the other hand, the proposed approach,

using stress-varying modulus of elasticity, had negligible impact on the cracking behavior even for beams with low reinforcement as expected. In other words, using stress-varying modulus of elasticity in Bischoff's (2005) equation did not make any difference from an engineering point of view (Figure 4).

Immediate deflections are mostly calculated under service loads. Therefore, the accuracy of deflection calculation is much more significant for loads at this level. The service load level for an RC beam approximately corresponds to 65% of the yielding load of the beam ( $P_y$ ) when gravity load and flexural resistance factors are considered in the design codes (ACI 318-19, 2019). Experimental  $P_y$  values were apparent and directly obtained from load-deflection curves of the test specimens (Figure 3). Experimental and analytical deflections correspond to experimental  $0.65P_y$  were considered service deflections ( $\delta_s$ ) and given in Table 3.

Branson (1965) and Bischoff (2005) equations gave the same results at the service loads for the RC beams with high and medium reinforcement ratios. On the other hand, Bischoff (2005) equation resulted slightly more deflections for the beams with low reinforcement. Nevertheless, both equations in their current form constantly underestimated the deflections for the service loads. They predicted almost 30% less than the experimental results for highly and medium reinforced beams. At low reinforcement ratios, this value was on average 22% and 14% less for Branson (1965) and Bischoff (2005), respectively. In other words, Bischoff (2005) correlated better with the experimental results. On the other hand, the proposed approach, using stress-varying modulus of elasticity, was in close agreement with the experimental results. The proposed approach estimated the deflection of the L75 specimen 23% more at service load levels. However, the overestimation was only 7% for specimen L100 which could be considered equivalent to L75. Thus, this contradiction was attributed to random causes arising from specific behavior of RC members. Nevertheless, it should not be disregarded that the deviation was in the safe region. When specimen L75 was excluded from the evaluation, the difference varied between +7% and -6%. Additionally, this range corresponded to deviations below 0.5 mm (Table 3).

**Table 3.** Service load deflections of specimens

Specimen	Experiment yield load, $P_y$ (kN)	Experiment $0.65P_y$ (kN)	Experiment $\delta_s$ (mm)	Branson $\delta_s$		Bischoff $\delta_s$		$\delta_s$ of the proposed approach	
				mm	Rel.	mm	Rel.	mm	Rel.
L75	28	18.2	5.2	4.2	0.81	4.8	0.92	6.4	1.23
M75	52	33.8	8.0	5.5	0.69	5.5	0.69	7.5	0.94
H75	82	53.3	9.1	6.6	0.73	6.6	0.73	9.4	1.03
L100	32	20.8	5.5	4.1	0.75	4.4	0.80	5.9	1.07
M100	61	39.7	8.3	5.8	0.70	5.8	0.70	8.2	0.99
H100	86	55.9	9.1	6.4	0.70	6.4	0.70	9.4	1.03

*Rel.: The ratio of the analytical deflection to the experimental deflection*

In the proposed approach, the best fit was observed in the behavior of medium reinforced beams. The curves almost overlap to the yield point. A similar favorable consistency was valid for specimen L100. In specimen L75, while the current approaches mostly underestimate the deflection, the proposed approach overestimate in the same proximity (Figure 4). The agreement between the experimental curves gradually decreased as they got closer to yield in highly reinforced RC beams. However, the proposed approach resulted deflections much more close to the experimental ones even in the yield regions. Moreover, slight deviations were on the conservative side (Figure 4).



#### 4. CONCLUSION

In this study, T-sectioned six RC beams with low, medium, and high reinforcements were tested and experimental load-deflection diagrams were obtained. Deflections were calculated according to Branson (1965) and Bischoff (2005) by using constant modulus of elasticity as it is recommended by ACI 318-14 (2014) and ACI 318-19 (2019), respectively. Afterwards, the nonlinear behavior of concrete that changes with stress was also taken into account for the Bischoff (2005) method to predict deflections as accurately as possible. The widely-accepted and practical Hognestad (1951) concrete stress-strain relationship was implemented in the proposed approach. Consistency between the analytical and experimental results was evaluated. In the current section, significant outcomes of the study were presented. On the other hand, it should be noted that the results are based on data from a limited number of test specimens. For this reason, solid and absolute judgements should be avoided.

When Branson (1965) and Bischoff (2005) equations were compared, Branson (1965) approach simulated the cracking behavior of RC beams with low reinforcement ratios better than Bischoff (2005). On the other hand, Bischoff (2005) approach was better for the tested medium and highly reinforced beams. Both deflection calculation methods did not result any significant difference under the assumed service loads and constantly underestimated the experimental deflections. The reached deviation was 30% less than the experimental results for high and medium reinforcement ratios.

Deflections could be calculated more accurately when non-linear stress-strain behavior of concrete was deployed in Bischoff (2005) approach. The proposed approach was able to estimate the experimental deflections under service loads with an average proximity of 5%. Moreover, this average value was on the safe side. The best fit to the experimental load-deflection curves was observed in medium reinforced beams which is valid for most of the case.

#### CONFLICT OF INTEREST

The author declares that there is no conflict of interest.

#### REFERENCES

- AASHTO. (2005). LRFD bridge design specifications, American Association of State Highway and Transportation Officials, USA.
- ACI 318-14. (2014). Building code requirements for structural concrete and commentary, American Concrete Institute, USA.
- ACI 318-19. (2019). Building code requirements for structural concrete and commentary. American Concrete Institute, USA.
- ACI 435R-95. (2000). Control of deflection in concrete structure. American Concrete Institute, USA.
- AS 3600-2009. (2009). Australian standard for concrete structures. Standards Australia, Australia.
- Ammash, H., Hemzah, S., & Al-Ramahee, M. (2018). Unified advanced model of effective moment of inertia of reinforced concrete members. *International Journal of Applied Engineering Research*, 13(1), 557-563.
- Arabshahi, A., Tavakol, M., Sabzi, J., & Gharaei-Moghaddam, N. (2022). Prediction of the effective moment of inertia for concrete beams reinforced with FRP bars using an evolutionary algorithm. *Structures*, 35, 684-705. doi:[10.1016/j.istruc.2021.11.011](https://doi.org/10.1016/j.istruc.2021.11.011)
- Bischoff, P. H. (2005). Reevaluation of deflection prediction for concrete beams reinforced with steel and fiber reinforced polymer bars. *Journal of Structural Engineering*, 131(5), 752-767. doi:[10.1061/\(ASCE\)0733-9445\(2005\)131:5\(752\)](https://doi.org/10.1061/(ASCE)0733-9445(2005)131:5(752))
- Bischoff, P. H. (2020). Comparison of existing approaches for computing deflection of reinforced concrete. *ACI Structural Journal*, 117(1), 231-240. doi:[10.14359/51718072](https://doi.org/10.14359/51718072)
- Branson, D. E. (1965). Instantaneous and time-dependent deflection on simple and continuous reinforced concrete beams (HPR Report No.7), Highway Department Bureau of Public Roads, USA.

- Carreira, D. J. & Chu, K. D. (1985). Stress-strain relationship for plain concrete in compression. *ACI Journal Proceedings*, 82(6), 797-804.
- CEB-FIB. (1970). International recommendations for the design and construction of concrete structures: principles and recommendations, Comité Euro-International-Federation Internationale de la Précontrainte, London, UK.
- CSA A23.3-04. (2004). Design of concrete structures, Canadian Standards Association, Canada.
- Desayi, P. & Krishnan S. (1964). Equation for the stress strain curve of concrete. *ACI Journal Proceedings*, 61(3), 345-350.
- Hognestad, E. (1951). A study of combined bending axial load in reinforced concrete members. University of Illinois Bulletin Series No. 399. The University of Illinois Engineering Experimental Station, USA.
- Hognestad, E., Hanson, N. W., & McHenry, D. (1955). Concrete stress distribution in ultimate strength design. *ACI Journal Proceedings*, 52(4), 455-480. doi:[10.14359/11609](https://doi.org/10.14359/11609)
- Kalkan, İ. (2010). Deflection prediction for reinforced concrete beams through different effective moment of inertia expressions. *International Journal of Engineering Research and Development*, 5(1), 72-80.
- Kim, S.-W., Han, D.-S., & Kim, K.-H. (2021). Evaluation of shear effect on deflection of RC beams. *Applied Sciences*, 11(16), 7690. doi:[10.3390/app11167690](https://doi.org/10.3390/app11167690)
- Kumar, P. A. (2004). Compact analytical material model for unconfined concrete under uni-axial compression. *Materials and Structures*, 37(9), 585-590. doi:[10.1007/BF02483287](https://doi.org/10.1007/BF02483287)
- Mancuso, C., & Bartlett, F. M. (2017). ACI 318-14 criteria for computing instantaneous deflections. *ACI Structural Journal*, 114(5), 1299-1310. doi:[10.14359/51689726](https://doi.org/10.14359/51689726)
- Popovics, S. A. (1973). Numerical approach to the complete stress-strain curve of concrete. *Cement and Concrete Research*, 3(5), 583-599. doi:[10.1016/0008-8846\(73\)90096-3](https://doi.org/10.1016/0008-8846(73)90096-3)
- Todeschini, C. E, Bianchini, A. C., & Kesler, C. E. (1964). Behavior of concrete columns reinforced with high strength steels. *ACI Journal Proceedings*, 61(6), 701-716.
- TS500. (2000). Requirements for design and construction of reinforced concrete structures, Turkish Standarts Institute, Turkey.